EXPERIMENTAL STUDY OF R-134A VAPORIZATION IN MINICHANNELS

Jacqueline Biancon Copetti, jcopetti@unisinos.br

Mario Henrique Macagnan, mhmac@unisinos.br

Nicole Luíse Froehlich Kunsler

Alisson de Oliveira
Universidade do Vale do Rio dos Sinos - Av. Unisinos, 950, 93022-000 – São Leopoldo, RS, Brazil

Abstract. *Evaporators of small and medium refrigeration systems, as in commercial and mobile air conditioning applications, are being studied to develop more compact and lighter equipments which reach a good thermal performance and reliability, with low pressure drop. In this way, evaporators are being designed with small tubes or channels and light materials. This work presents the results of an experimental study to characterize heat transfer and pressure drop during evaporation in a horizontal tube. An experimental apparatus was developed where the refrigerant, in a closed circuit, is vaporized under different conditions. The test section was made of a stainless steel tube with effective heating length of 185 mm and channel diameter of 2.6 mm. The experimental conditions including operating temperature, mass flow rate and heat flux to the test section were set to the desired values. Heat fluxes range from 10 to 100 kWm^{-2}, and mass velocities were set to discrete values in the range of 240-1200 $kgm^{-2}s^{-1}$ and saturation temperature of 22°C for R-134a. The study analyzed the heat transfer, through the local heat transfer coefficient along the flow and pressure drop. It was possible to observe the significant influence of heat flux in the heat transfer coefficient and pressure drop. Some flow patterns observed in the experiments were also presented.*

Keywords*: flow boiling, minichannels, heat transfer coefficients, R-134a*

1. INTRODUCTION

Evaporators of small and medium refrigeration systems, as in commercial and mobile air conditioning applications, are being studied to develop more compact and lighter equipments which reach a good thermal performance and reliability, with low pressure drop. In this way, the evaporators are being designed with small tubes or channels and light materials, like aluminum. Due to the increase in use of this compact two phase heat exchangers, the investigation of flow boiling heat transfer and pressure drop in small channels have become more important in recent years.

In the last two decades, theoretical and experimental studies of boiling in small channels are growing, as can be seen in Kandlikar (2002) and Thome et. al (in Hewitt, 2002). The difference between small diameter channels, mini and microchannels, is not clearly defined in the literature. Kandlikar (2002), for example, used an arbitrary classification based on the hydraulic diameter: conventional channels to hydraulic diameters greater than 3 mm; minichannels to hydraulic diameters between 200 μm and 3 mm and microchannels, between 10 and 200 μm. Thome et. al (in Hewitt, 2002) discussed some criteria to define these limits. One criterion could be the bubble diameter in relation to the channel diameter in such a way that the bubble growth is confined by the size of the channel, existing just one bubble in the channel cross-section. However, this classification depends on the refrigerant flow pressure. Another criterion is the use of the confinement number, as defined by Kew and Cornwell (1997). For confinement numbers greater than 0.5, the heat transfer and flow characteristics could be significantly different than those observed in macrochannels.

This definition is important because with the decrease of hydraulic diameter, the surface tension predominates over gravity forces and some flow patterns observed in macro scales experiments do not exist in micro scales.

According to Vlasie (2004), heat transfer, pressure drop and flow regimes for two-phase flow in small channels can not be adequately predicted by the existing correlations for macrochannels. The boiling heat transfer of refrigerants in macrochannels is controlled by the convection mechanism for vapor qualities greater than 20 to 30%. For small diameter channels, the process is dominated by nucleate boiling, convective boiling or both mechanisms. Studying the effect of tube diameter on boiling heat transfer for R-134a, Saitoh et. al (2005) observed that for a 3.1 mm ID tube, the heat transfer coefficient increased with the increase in mass velocity or heat flux. For a 0.51 mm ID tube, the heat transfer coefficient also increased for greater heat flux, but it was not significantly affected by the increase in mass velocity. The contribution of forced convective evaporation to the boiling heat transfer decreases with decreasing tube diameter. Another feature observed was that when the flow pattern changes from continuous flow (annular flow) to intermittent flow (slug or plug flow), the heat transfer coefficient decreased at high vapor quality. Similar results were found by Tibiriçá and Ribatski (2009) studying boiling heat transfer for R-134a on a horizontal tube of 2.32 mm ID.

In this paper are reported some experimental results of R-134a two-phase flow boiling, heat transfer and pressure drop in a horizontal stainless steel minichannel of 2.62 mm ID. Results are discussed in terms of the effects of intervening physical parameters like heat flux, mass velocity and vapor quality.

2. EXPERIMENTAL ASPECTS

2.1. Facility and instrumentation

A test rig was constructed to investigate flow boiling and pressure drop in electrically heated horizontal mini channels. The details of this rig are shown schematically in Fig. 1. The rig consists of two loops to provide controlled flow of refrigerant. The main loop has a Coriolis mass flow meter (02), a pre-heater section (04), the test section (05) and the visualization section (06). The secondary loop consists of a condenser (08), a refrigerant reservoir, a dryer filter (09), a volumetric pump (01) and a subcooler (03). The condenser and the subcooler have independent circuits, using the ethylene-glycol/water solution as secondary refrigerant. Each circuit is controlled by a thermal bath with constant temperature, according Fig. 2. This set up permits to control the refrigerant saturation temperature.

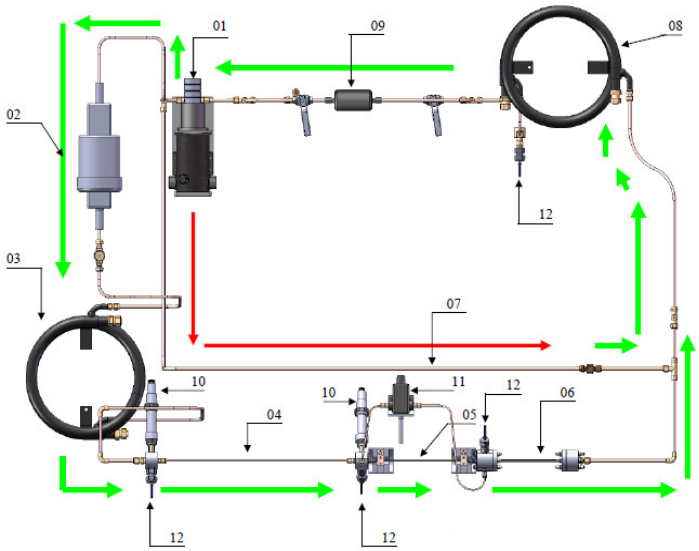

Figure 1. Schematic representation of test rig.

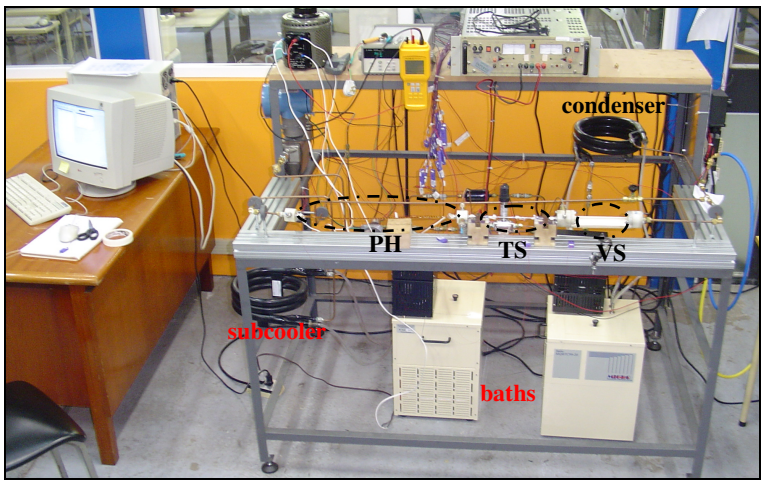

Figure 2. View of the experimental rig with the thermostatic baths under the bench.

In the main loop of the circuit the pre-heater (PH) permits to establish the experimental conditions in the test section. It consists of a horizontal cooper tube with length of 445 mm heated by electrical tape resistance (11.7 Ωm^{-1}) uniformly

wrapped around on its external surface to guarantee a uniform heat flux to refrigerant. The electrical resistance is insulated from the tube with a kapton conductive tape. In the pre-heater the power is adjusted by a voltage converter. The test section (TS) consists of a smooth horizontal stainless steel tube with effective length of 183 mm and 2.62 mm ID and is uniformly heated by direct application of electrical current in the tube wall (Joule effect), controlled by a power supply. After the test section there is a visualization section (VS) with a 158 mm length glass tube with the same test section internal diameter. The pre-heater and test section are thermally insulated.

The refrigerant enters in the preheating section as subcooled liquid and the saturation condition on the exit of the pre-heater, or the vapor quality, varies according to the heat flux. A liquid visor before the pre-heater entrance makes possible to control the physical state of refrigerant. The liquid reservoir is used for improving the stabilization of the refrigerant flow. The pressure measurements in the inlet and outlet of the pre-heater were carried out by two absolute transducers (Fig.1 - 10) and the temperatures by 0.076 mm thermocouples (Fig.1 - 12) type E, in direct contact to refrigerant flux.

The refrigerant vaporizes along the test section. Refrigerant temperatures are measured in the inlet and outlet of this section (Fig. 3 - 06), as well as the tube wall temperatures, as it is possible to see in Fig. 3. The tube wall thermocouples are type E of 0.076mm directly fixed by a thermally conductive paste. The position of each thermocouple is described in Fig. 4 (a) and (b). In the three central positions of tube there are four thermocouples in each position, separated by 90° one of the other, according Fig. 4 (a). In the entrance and exit of the tube are fixed two thermocouples on the wall, in the upper and bottom parts (Fig 4 (b)). In the test section the differential pressure transducer (Fig.3 – 05) allows the determination of the exit pressure.

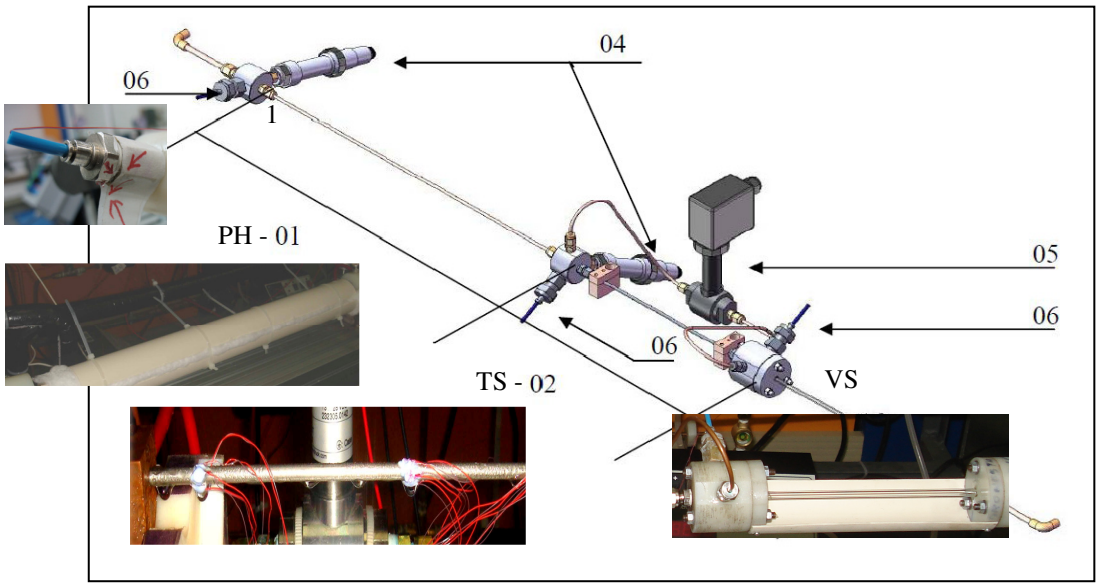

Figure 3. Details of pre-heater, test and visualization sections.

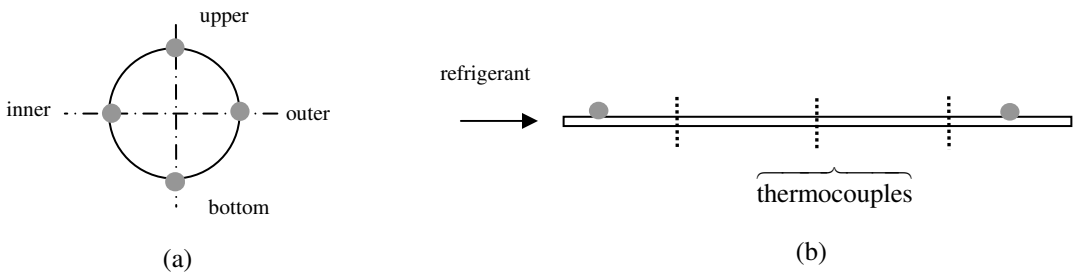

Figure 4. Thermocouples position in the tube wall of test section.

The flow pump rate is controlled by a frequency inverter and a bypass piping line after pump allows setting more precise flow rate through a needle-valve, as detailed in Fig.1 – 07.

The pressure transducers, thermocouples, mass flow and power meter were connected to an acquisition data system composed by a multimeter (Agilente, model 34970), connected to a microcomputer by a RS232 interface. Software BenchLink Data Logger from Agilent was used to data monitoring and acquisition.

2.2. Measurements procedures and data reduction

2.1. Experimental conditions

Many tests were carried out with the aim of verifying the thermal and hydraulic behaviour during vaporization of R134a in a 2.62mm ID tube for different refrigerant flow rates and heat flux. Experimental test conditions are shown in Tab. 1. The vapor quality condition in the entrance of test section for each test was reached by different heating powers in the pre-heater.

Table 1. Test conditions.

Test section heat flux (q"s) [kW/m^2]	10, 20, 33, 47, 67, 87 and 100
Mass velocity (G) [kg/sm^2]	240, 450, 550 and 740
Saturation temperature (Tsat) [°C]	22
Pre-heater heating power [W]	45 to 270

2.2. Data reduction

The vaporization parameters, including vapor quality, internal wall temperature, saturation temperature and the heat transfer coefficient, were calculated from measured data of refrigerant temperatures, wall temperature in the test section, pressures, flow rate, heat flux and geometrical parameters. The thermodynamic properties of R-134a were obtained from REFPROP software (Lemmon et. al, 2007).

The heat transfer coefficient calculation supposed the following considerations:

- The heat loss to the surroundings can be neglected.
- Heat transfer in the axial direction can be neglected.
- Volumetric heat generation, and hence heat flux, is uniform along the tube in the test section.
- Pressure drop from the saturation point to outlet pressure is a linear function of tube length.

The vapor quality in the entrance of test section was calculated from energy balance in the pre-heater and the enthalpies were estimated through pressure and temperature measurements downstream and upstream of the section. The exit enthalpy in the test section was estimated in the same way than in the pre-heating section.

The local heat transfer coefficient, h_z, was determined using the Eq. (1).

$$h_z = \frac{q''}{T_{w_i} - T_{sat}} \tag{1}$$

where q" is the heat flux, T_{w_i} is the inner wall temperature and T_{sat} is the saturation temperature at a local refrigerant pressure calculated by interpolation between the inlet and outlet pressures. The heat flux is calculated as the ratio between the electrical power and the internal area for the heated length. The T_{w_i} was calculated assuming radial conduction through the wall, subject to internal heat generation as given by Eq. (2).

$$T_{w_i} = T_{w_o} + \frac{\dot{q}}{4k}\left(r_o^2 - r_i^2\right) - \frac{\dot{q}}{2k} r_o^2 \ln\left(\frac{r_o}{r_i}\right) \tag{2}$$

where $\dot{q}$ is the volumetric heat generated, T_{w_o} is the external wall temperature, k is thermal conductivity and r_o and r_i the external and internal radios, respectively. For each axial location z along the test tube, the external wall temperature is the average of measured temperatures around the cross section, like shown in Fig. 4 and calculated by Eq. 3.

$$T_{w_o} = \frac{T_{w_{top}} + T_{w_{side_i}} + T_{w_{side_o}} + T_{w_{botton}}}{4} \tag{3}$$

3. RESULTS AND DISCUSSION

3.1. Effect of mass velocity and heat flux on heat transfer coefficient\

Figures 5a-d shows the effect of heat flux on heat transfer coefficient for different mass velocity. It is possible to verify the dependence of the heat transfer coefficients on the heat flux, mainly at the low quality region (quality less than 40%). The heat transfer coefficient increased with increasing heat flux. Many authors (Choi et al., 2007 and Lin et. al, 2001) have associated this behavior to nucleate boiling in the initial part of evaporation, mainly under high heat flux. This condition will tend to be suppressed at high vapor quality where the effect of heat flux on heat transfer coefficient becomes lower and the coefficient decreases, as can be observed in Figs. 5a and 5b. Figure 5a also shows that for low mass velocity (G=240 kg/sm^2), the low heat flux (q"=5 kW/m^2) almost does not affect the heat transfer coefficient.

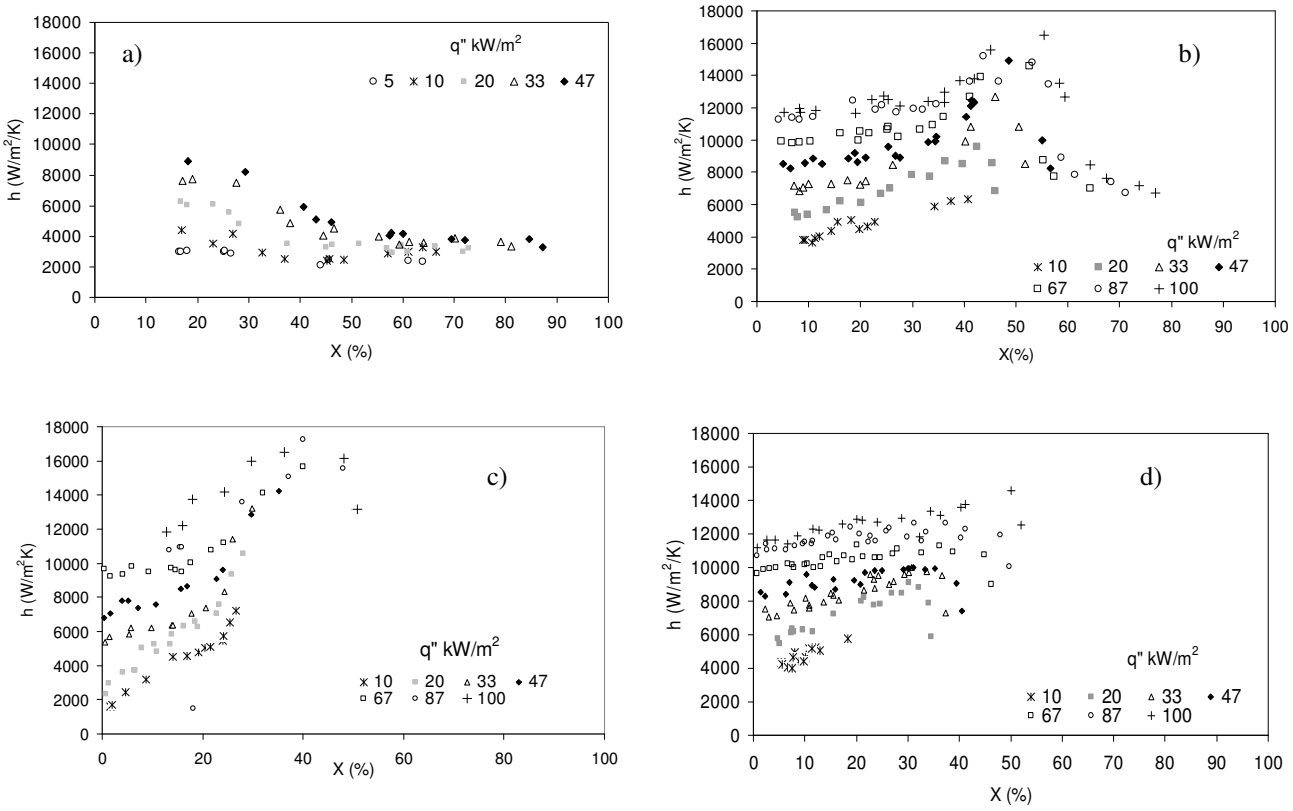

Figure 5. Effect of heat flux on heat transfer coefficient for different mass velocities: a) G=240, b) G=440, c) G=550 and d) G=740 kg/sm^2 for Tsat=22°C.

The effect of mass velocity on heat transfer coefficient is shown in Figs. 6a-b. The effect of mass velocity is almost insignificant at the low vapor quality region. This result can also be related to a nucleate boiling condition.

The convective boiling heat transfer contribution appears for higher mass velocity which results in greater heat transfer coefficient at moderate vapor quality. The decrease in the heat transfer coefficient occurs at a lower quality for higher mass flux. The lower mass velocity condition results show smaller increases in the heat transfer coefficient in the convective region.

3.2. Flow patterns

The heat transfer coefficient behavior can also be explained by flow regimes. According Coleman and Garimella (1999), Tibiriçá and Ribastki (2009), the flow regimes and patterns are classified as: stratified (smooth and wavy patterns), intermittent (elongated bubble and slug patterns), annular (wavy and annular patterns) and dispersed (bubble and dispersed patterns). In Fig. 7a-g, are shown the flow patterns observed during the tests. These images were recorded in the glass visualization section with a digital high speed camera.

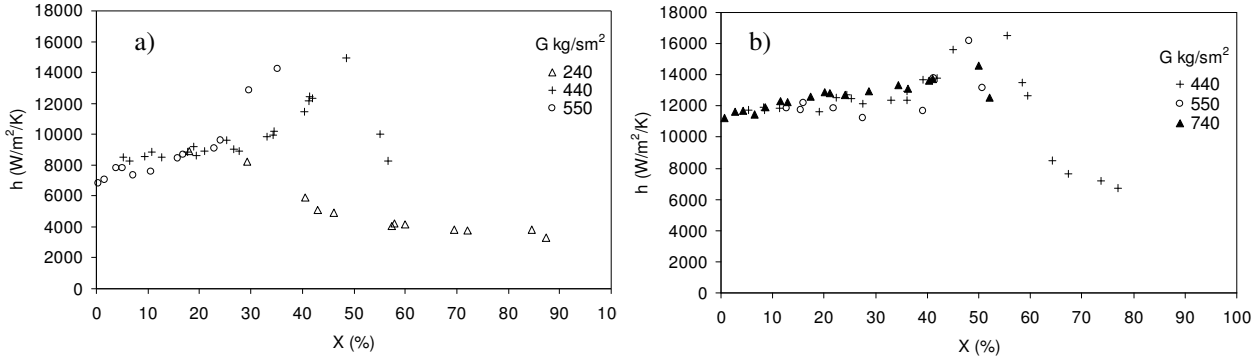

Figure 6. Effect of mass velocity on heat transfer coefficient for different heat flux:
a) q"=47 kW/m^2, b) q"=100 kW/m^2.

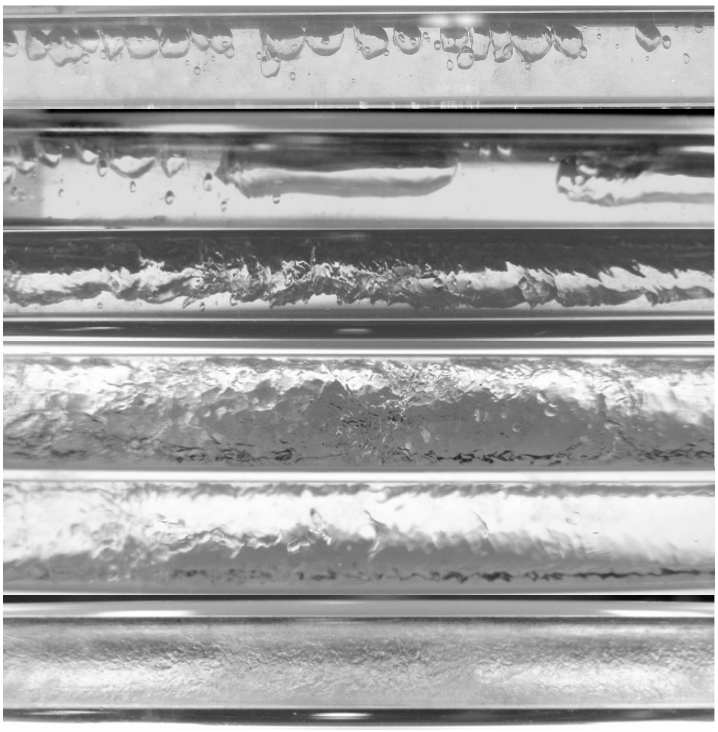

a) G= 1280 kg/m²s x=2.9% (bubble)

b) G= 740 kg/m²s x=7.7% (elongated bubble)

c) G= 550 kg/m²s x=12.1% (stratified)

d) G= 550 kg/m²s x=33.2% (annular-wavy)

e) G= 440 kg/m²s x=45% (annular-wavy)

f) G= 740 kg/m²s x=52 % (annular)

Figure 7. Flow pattern visualizations for R-134a, 2.62 mm tube and Tsat=22°C.

3.3. Pressure drop

The pressure drop measured in the test section as function of vapor quality for different heat flux and mass velocity is shown in Fig. 8 a-c. The test section, constructed with a horizontal stainless steel tube of 2.62 mm ID has an internal surface roughness of 2.05 μm (Ra), measured with a Pantec rugosimeter.

The pressure drop for small diameter tubes is affected by the flow regime transitions. As can be seen, the pressure drop increases with the vapor quality independent of other parameters. The pressure drop increases with increasing heat flux for the same mass velocity (as shown in Fig. 8a). With decreasing of mass velocity, the pressure tends to remain almost constant, as can be seen in Fig. 8b and c, for G = 240 kg/m^{2}s. Similar trends were presented by Ould Didi, et. al (2002) for refrigerants flow in tubes of 10.92 to 12 mm and by Tran et. al (1999), for small channels.

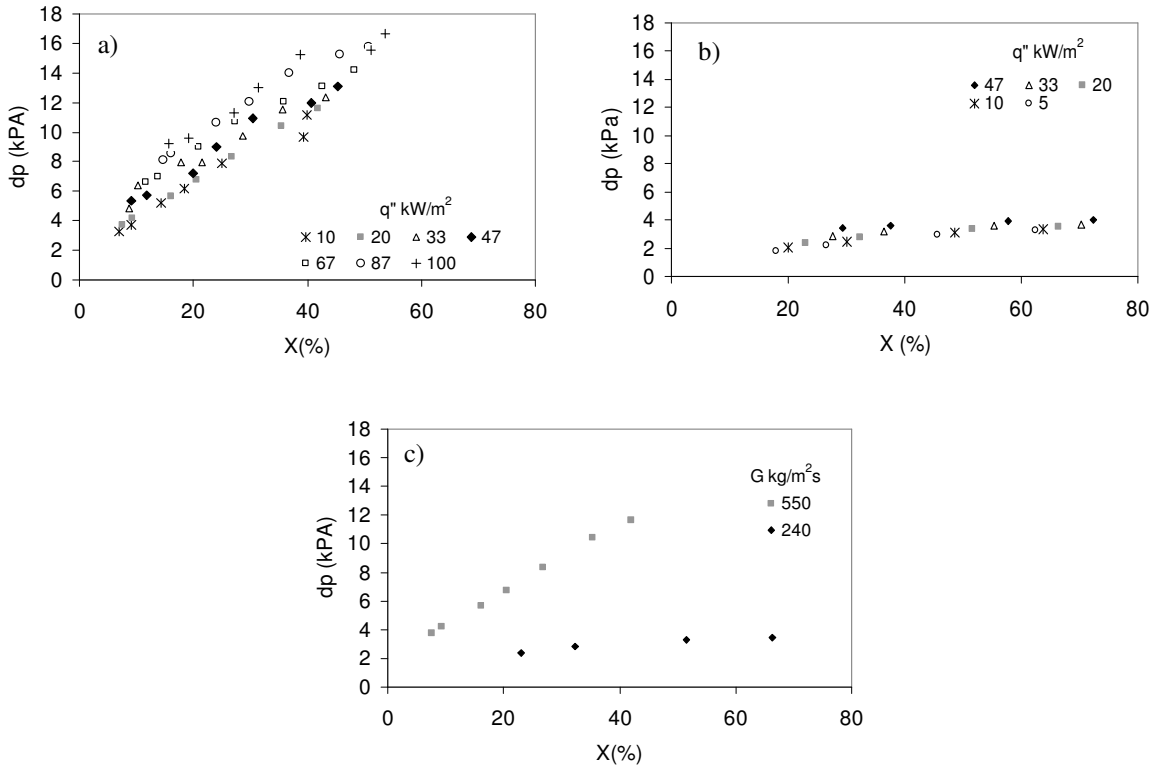

Figure 8. Effect of heat flux on pressure drop a) G=550 and b) 240 kg/sm^2 and c) effect of mass velocity on pressure drop for heat flux 20 kW/m^2 .

4. CONCLUSIONS

Preliminary results of experimental two-phase flow of R-134a in horizontal minichannel are presented. It was observed the dependency of heat transfer coefficient on heat flux and mass velocity. The heat transfer coefficient increased with increasing heat flux and mass velocity, but strong heat flux dependence was observed, mainly to lower vapor quality region.

Comparing the results and observations made from different researches regarding boiling mechanisms in small diameter channels many uncertainties and contradictions still exist. However, the results indicated that the nucleate boiling mechanism seems to be dominant one.

In the pressure drop results it was possible to verify that the effects of heat flux and mass velocity are also important, however it should be more investigated due to influence in evaporators design.

The flow regimes were observed during experiments and the bubble, slug and annular flow patterns were identified.

5. ACKNOWLEDGEMENTS

The authors gratefully acknowledge CNPq, Conselho Nacional de Desenvolvimento Científico e Tecnológico for the financial support for this work, under contract #476843/2006-5. Kunsler, N.L.F. was supported by grant from Fundação de Amparo a Pesquisa do Rio Grande do Sul (FAPERGS) and Oliveira, A. was supported by grant from UNISINOS. The authors grateful to Professor Júlio Passos, from Universidade Federal de Santa Catarina (UFSC), for his comments and suggestions on experimental work.

6. REFERENCES

Choi, K., Pamitran, A.S., Oh, C.Y., Oh, J.T., 2007, "Boiling heat transfer of R-22, R-134a and CO_2 in horizontal smooth minichnnels", International Journal of Refrigeration, Vol. 30, pp. 1336-1346.

Coleman, J.W., Garimella, S., 1999, "Characterization of two-phase flow patterns in small diameter round and rectangular tubes", International Journal of Heat and Mass Transfer, Vol.42, pp. 2869-2881.

Hewitt, G. F. Ed., 2002, "Handbook of heat exchanger design", New York: Begell House, 1200 p.

Kandlikar, S.G., 2002, "Fundamental issues related to flow boiling in minichannels and microchannels", Experimental Thermal and Fluid Science, Vol.26, pp. 389-407.

Kew, P., Cornwell, K., 1997, "Correlations for prediction of boiling heat transfer in small diameter channels", Applied Thermal Engineering, Vol.17, pp. 705-715.

Lemmon, E.W., Huber, M.L., McLinden, M.O. "NIST Standard Reference Database 23: Reference Fluid Thermodynamic and Transport Properties-REFPROP, Version 8.0", National Institute of Standards and Technology, Standard Reference Data Program, Gaithersburg, 2007.

Lin, S., Kew, P.A., Cornwell, K., 2001, "Two-phase heat transfer to a refrigerant in a 1 mm diameter tube", International Journal of Refrigeration, Vol.24, pp. 51-56.

Ould Didi, M.B., Kattan, N., Thome, J.R., 2002, "Prediction of two-phase pressure gradients of refrigerants in horizontal tubes", International Journal of Refrigeration, Vol. 25, pp. 935-947.

Saitoh, S., Daiguji, H., Hihara, E., 2005, "Effect of tube diamenter on boiling heat transfer of R-134a in horizontal small-diamenter tubes", Internation Journal of Heat and Mass Transfer, Vol.48, pp. 4973-4984.

Tibiriçá, C.B., Ribatski, G., 2009, "An experimental study in micro-scale flow boiling heat transfer", Proceedings of the ECI International Conference on Boiling Heat Transfer, Florianópolis, Brazil.

Tran, T.N., Chyu, M.C., Wambsganss, M.W., France, D.M., "Two-phase pressure drop of refrigerants during flow boiling in small channels: an experimental investigation and correlation development", Proceedings of the International Conference on Compact Heat Exchangers and Enhancement Technology for the Process Industries, Banff, Canada, 1999.

Vlasie, C., Macchi, H., Guipart, J., Agostini, B., 2004, "Flow boiling in small diameter channels", International Journal of Refrigeration, Vol.27, pp. 191-201.

7. RESPONSIBILITY NOTICE

The authors are the only responsible for the printed material included in this paper.